Abietadiene Synthase Catalysis: Conserved Residues Involved in Protonation-Initiated Cyclization of Geranylgeranyl Diphosphate to (+)-Copalyl Diphosphate†

Reuben J. Peters and Rodney B. Croteau*

Institute of Biological Chemistry, Washington State University, Pullman, Washington 99164-6340

Received October 3, 2001; Revised Manuscript Received December 10, 2001

ABSTRACT: Abietadiene synthase catalyzes two sequential, mechanistically distinct cyclization reactions in the formation of a mixture of abietadiene double bond isomers as the committed step in resin acid biosynthesis. Each reaction is carried out at a separate active site residing in a structurally distinct domain, and the reactions are kinetically separable. The first cyclization reaction is initiated by protonation of the terminal double bond of the universal diterpene precursor, geranylgeranyl diphosphate. The pH dependence of the overall reaction is consistent with an acid−base catalytic mechanism, and a divalent metal ion plays a role in this reaction probably by binding the diphosphate moiety to assist in positioning the substrate for catalysis. A putative active site for the protonation-initiated cyclization was defined by modeling abietadiene synthase and locating the DXDD motif previously shown to be involved in this reaction. A number of charged and aromatic residues, which are highly conserved in mechanistically related diterpene cyclases, line the putative active site. Alanine substitutions were made for each of these residues, as were asparagine and glutamate substitutions for the aspartates of the DXDD motif. Kinetic evaluation confirmed the involvement of most of the targeted residues in the reaction, and analysis of mutational effects on the pH−activity profile and affinity for a transition state analogue suggested specific roles for several of these residues in catalyzing the cyclization of geranylgeranyl diphosphate to (+)-copalyl diphosphate. A functional role was also suggested for the cryptic insertional element found in abietadiene synthase and other diterpene synthases that carry out similar protonation-initiated cyclizations.

Secretion of oleoresin, a mixture of monoterpene olefins (turpentine) and diterpene resin acids (rosin), is a primary response of conifers to wounding (*1*). Following secretion, volatilization of the turpentine carrier results in solidification of the nonvolatile resin acids which seals the wound (*2*). Most resin acids of grand fir (*Abies grandis*) are derived from abietadiene positional isomers, which undergo subsequent oxidation of the C18 methyl group to a carboxyl function (see Scheme 1) (*3*, *4*). Abietadiene synthase (AS)[1] from grand fir catalyzes the conversion of the universal diterpene precursor geranylgeranyl diphosphate (GGPP, **1**) to a mixture of abietadiene double bond isomers as the committed step of resin acid (e.g., abietic acid, **5**) biosynthesis (*4*, *5*). To form the tricyclic perhydrophenanthrene-type structure, AS catalyzes two sequential, mechanistically different cyclizations (Scheme 1), with each reaction occurring at a distinct active site (*6*). The first cyclization is initiated by protonation across the terminal C14−C15 double bond of GGPP, and is terminated by deprotonation to produce the stable bicyclic intermediate (+)-copalyl diphosphate (CPP, **2**). This reaction is analogous to that catalyzed by (−)-copalyl diphosphate synthase (kaurene synthase A) of the gibberellin biosynthetic pathway (*7*, *8*). In the second reaction, ionization of diphosphate ester **2** initiates formation of the third ring and is coupled, via intramolecular proton transfer within a sandaracopimarenyl intermediate (**3**), to a 1,2-methyl migration that creates the C13 isopropyl group characteristic of the abietane skeleton (e.g., abietadiene, **4**). Such ionization-initiated cyclization reactions are common in terpene biosynthesis (*9*).

The protonation-initiated cyclization to CPP has been shown to involve addition of an external proton to C14 of GGPP followed by removal of a proton from the C19 methyl group of the substrate (*10*). Kinetic analysis has demonstrated that the intrinsic rate-determining step of the overall reaction occurs after formation of CPP (i.e., k_{cat} is the same with either GGPP or CPP as the substrate) (*5*). However, the *observed* rate with GGPP never approaches the maximum rate that can be attained with CPP due to substrate inhibition of the protonation-initiated cyclization step (Figure 1) (*6*). Therefore, the *observed* rate of the overall reaction from GGPP is limited by the initial cyclization step, while that from CPP is limited by the intrinsic rate-determining step; the two reactions can, therefore, be separately analyzed. A transition state analogue of the initial carbocationic intermediate formed

† This work was supported by National Institutes of Health Grant GM31354 to R.B.C. and by a Postdoctoral Fellowship from the Jane Coffin Childs Memorial Fund for Medical Research to R.J.P.

* To whom correspondence should be addressed. Phone: (509) 335-1790. Fax: (509) 335-7643. E-mail: croteau@wsu.edu.

[1] Abbreviations: AS, abietadiene synthase [the prefix r denotes the recombinant "pseudomature" (truncated) enzyme]; CPP, copalyl diphosphate; GC, gas chromatography; GGPP, (*E*,*E*,*E*)-geranylgeranyl diphosphate; K_{si}, substrate inhibition constant; MS, mass spectrometry; PCR, polymerase chain reaction; WT, wild-type rAS; 5-EAS, 5-*epi*-aristolochene synthase.

10.1021/bi011879d CCC: $22.00
Published on Web 01/12/2002

Scheme 1: Biosynthetic Conversion of Geranylgeranyl Diphosphate (**1**), via (+)-Copalyl Diphosphate (**2**) and a Sandaracopimarenyl Intermediate (**3**), to Abietadiene (**4**) and Abietic Acid (**5**)[a]

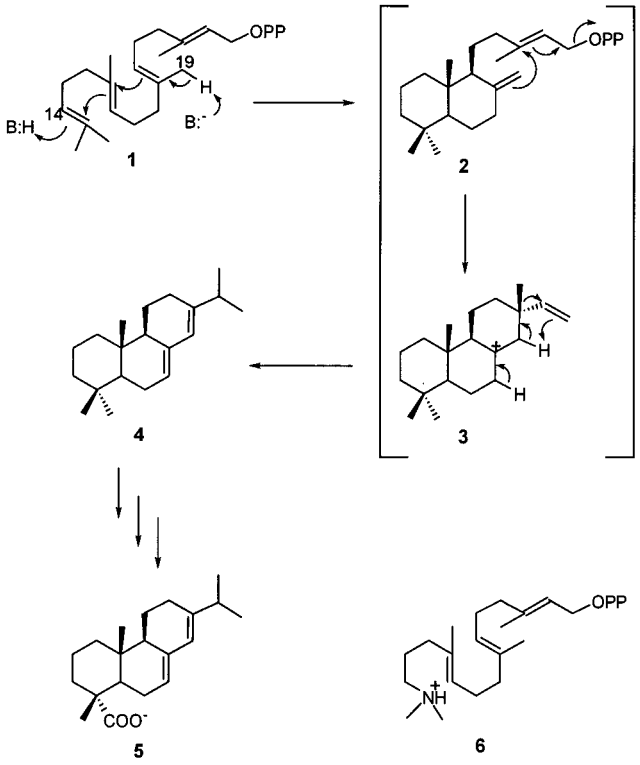

[a] The structure of 14,15-dihydro-15-azageranylgeranyl (**6**) is also shown.

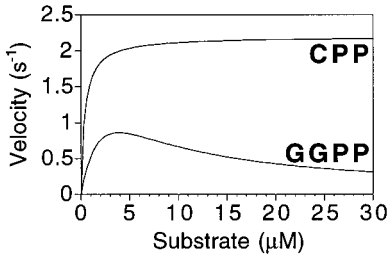

FIGURE 1: Kinetic analysis of rAS demonstrates substrate inhibition with GGPP but not with CPP (*5*). The calculated k_{cat} is the same for either substrate (see Table 1), but the observed rate of production of abietane olefins from GGPP never approaches that observed from CPP due to substrate inhibition.

by protonation, 14,15-dihydro-15-azageranylgeranyl diphosphate (**6**, 15-aza-GGPP; $K_i^{GGPP} = 0.2$ nM), is bound by AS much more tightly than the substrate ($K_M^{GGPP} = 3\ \mu$M), thus demonstrating enzymatic stabilization of this initial high-energy intermediate and providing a probe for this active site (*6*).

Aspartate-rich substrate binding motifs are known to play important roles in terpenoid cyclizations (*9*) and in mechanistically related prenyl transfer reactions (*11*). The $DXDD_{402-405}$ element in the N-terminal domain of AS is required for the protonation-initiated cyclization of GGPP to CPP, and the $DDXXD_{621-625}$ element in the C-terminal domain is required for the diphosphate ionization-initiated cyclization and rearrangement of CPP to abietadienes (Figure 2). Thus, alanine substitution for Asp404 or for Asp621 prevents the corresponding cyclization (*6*). Here, we present a more complete analysis of the protonation-initiated cyclization catalyzed in the N-terminal domain. Cyclization proceeds via an acid−base catalytic mechanism, and the pH dependence of the reaction rate implies that both the acid and base are involved in the rate-limiting step. In addition, a role is demonstrated for a divalent metal ion cofactor in this reaction mechanism. Finally, mutational analysis of the putative active site for this reaction, identified by locating the DXDD motif in a modeled structure of AS, suggests possible roles for several residues, all of which are also conserved in other diterpene synthases catalyzing similar protonation-initiated cyclization reactions.

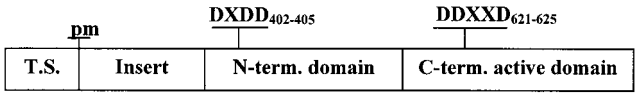

FIGURE 2: Schematic diagram of abietadiene synthase illustrating general structural features and the locations of the aspartate-rich elements. T.S. represents the transit sequence. The unusual insertional element of AS (Insert) and related terpenoid synthases has been described previously (*15*, *16*). The overall structure is modeled on 5-*epi*-aristolochene synthase (*13*). Numbering is based on the preprotein [i.e., the pseudomature (pm) recombinant enzyme starts with Met and then Val85−Ala868].

EXPERIMENTAL PROCEDURES

Materials and General Procedures. Liquid scintillation counting and product analysis by GC−MS were carried out as previously described (*4*, *12*). The preparations of (*E*,*E*,*E*)-[1-^{3}H]geranylgeranyl diphosphate (120 Ci/mol) (*4*) and of (+)-[1-^{3}H]CPP (120 Ci/mol) (*5*) have been described elsewhere. The crystal structure of tobacco 5-*epi*-aristolochene synthase (5-EAS) is the only plant terpene cyclase structure currently available (*13*); therefore, a modeled structure for AS was generated using 5-EAS as the scaffold with energy minimization performed using Gromos96 (*14*).

Enzyme Assays. Kinetic assays with freshly prepared enzyme were performed as previously described (*5*). The reaction time and concentration of rAS were scaled to permit measurement of mutant enzymatic activity; for impaired mutants, the reported kinetic constants are accurate to within ±50% based on replicated assays. Tight binding inhibition exhibited by 15-aza-GGPP limited analysis of this analogue to the determination of apparent inhibition constants by Dixon plotting, as previously described (*6*). To evaluate the influence of pH, 50 mM Bis-Tris propane was substituted for the original Hepes buffer (*5*) to broaden the effective buffering range. To examine the requirement for a divalent metal ion cofactor, 2.5 mM EDTA was substituted for both $MgCl_2$ and $MnCl_2$ in the normal assay buffer, and kinetic analysis was performed in the presence of EDTA. To assess the production of CPP in the absence of a divalent metal ion, protonation-initiated cyclization catalysis was terminated by adding the selective inhibitor 15-aza-GGPP (0.1 μM) (*6*), followed by the addition of 10 mM $MgCl_2$ to allow the conversion of any CPP that was produced to olefinic products, which were measured as described previously (*5*). To monitor possible formation of alternative or abortive diphosphate esters by mutant enzymes, assay mixtures were treated with acid as previously described (*6*) to solvolyze these products (to the corresponding alcohols) which were analyzed by GC−MS.

Mutant Construction and Expression. Point mutants were constructed from the wild-type rAS gene using a previously

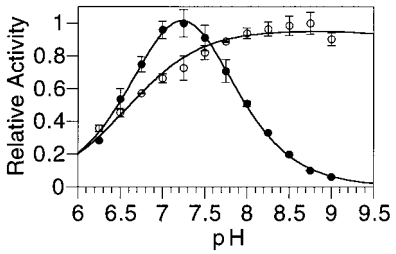

FIGURE 3: Differential pH dependence of abietadiene synthase activity with either GGPP (●) or CPP (○) as the substrate. Relative activities for the overall reaction (from GGPP), reflecting protonation-initiated cyclization, and for only the ionization-initiated cyclization (from CPP) are plotted (error bars indicate the standard deviation of duplicate measurements).

described overlapping fragment PCR scheme (*6*) in which complementary mutagenic primers were used to produce two overlapping fragments containing the introduced mutation, which were then recombined to produce the full-length mutated gene. Mutant and wild-type rAS were expressed in *Escherichia coli* BLR (Stratagene) at 15 °C in 1 L NZY cultures, and were purified as previously described (*5*). The concentration of purified rAS was determined by absorbance at 280 nm using the calculated extinction coefficient (138 350 M^{-1} cm^{-1}).

RESULTS

pH−Activity Profile of Abietadiene Synthase. The reactions of AS with GGPP and CPP are kinetically separable due to the substrate inhibition observed with GGPP. Because this inhibition occurs at the active site for protonation-initiated cyclization, it reduces the amount of productive enzyme−substrate complex formed (*6*). Therefore, although the intrinsic rate-limiting step resides after formation of CPP (*5*), the *observed* rate (k_{obs}) for the overall reaction with GGPP reflects that of the protonation-initiated cyclization step. In practice, this feature can allow dissection of external influences on the protonation-initiated cyclization relative to the diphosphate ionization-initiated cyclization and rearrangement, assuming that the K_M/K_i (i.e., the ratio of productive vs nonproductive enzyme−substrate complexes) for GGPP remains approximately constant.

The pH dependence of AS activity (k_{obs}) shows clear differences between the reaction with GGPP and CPP as the substrate (Figure 3). Unfortunately, because the level of substrate inhibition by GGPP decreases with increasing pH, the determined ionization constants (pK_a) reflect a complex mixture of effects on binding (both productive and nonproductive) and catalysis, rather than the specific ionization constants for participating acid and base groups. Nonetheless, it is clear that the rate of cyclization of GGPP exhibits a pH dependence typical of an acid−base catalytic mechanism. This somewhat surprising result suggests a change in the rate-determining step, from base- to acid-dependent with increasing pH, or that both the acid and base are involved in the slow step or in stabilizing a single transition state in this bicyclization reaction. Maxium activity occurs at an optimum pH of 7.2 and is rapidly lost with either decreasing or increasing pH, presumably reflecting, at least in part, protonation of the base (proton acceptor) leading to loss of activity with decreasing pH ($pK_a \sim 7.0$), or deprotonation of the acid (proton donor) resulting in loss of activity with increasing pH ($pK_a \sim 7.5$). In contrast to the results with GGPP as the substrate, the pH-dependent activity profile with CPP as the substrate in the second reaction exhibits quite different behavior, with a much higher optimum pH (8.7 vs 7.2) and activity over a much broader pH range (Figure 3); this behavior likely reflects the quite different catalytic mechanism of the diphosphate ionization-initiated cyclization and rearrangement step.

Divalent Metal Ion Dependence. The overall reaction catalyzed by AS requires a divalent metal ion cofactor (*4*), and it was shown that the second step, from CPP to abietadienes, exhibits an absolute dependence on a divalent metal ion cofactor (Table 1), as do most other diphosphate ester ionization-dependent terpene synthases (*9*). To determine if there is a role for a divalent metal ion in the protonation-initiated cyclization, it was therefore necessary to differentiate the second, ionization-dependent, step from the first, protonation-initiated, step. The level of production of CPP in the absence of any divalent metal ions was determined by adding 0.1 μM 15-aza-GGPP to specifically terminate further protonation-initiated cyclization (K_i^{GGPP} = 0.2 nM; K_i^{CPP} = 20 μM); subsequent addition of 10 mM $MgCl_2$ selectively enabled the conversion of CPP to abietadienes (i.e., without further cyclization of GGPP to CPP), which are easily assessed following extraction into an organic solvent. The altered kinetic constants for this first cyclization, determined in the absence of divalent metal ions ($K_M \sim 20$ μM and $k_{cat} = 2 \times 10^{-3}$ s^{-1}, without observable substrate inhibition), clearly demonstrated that divalent metal ions play a role in both the productive and nonproductive binding of GGPP, as well as in catalysis of the protonation-initiated cyclization step. However, this first reaction is not completely dependent on the presence of divalent metal ions ($k_{cat} \sim 10^{-3}$ s^{-1}), in contrast to the absolute requirement for divalent metal ions in the diphosphate ester ionization-initiated step ($k_{cat} \sim 10^{-5}$ s^{-1}).

Mutational Analysis of a Putative Active Site. The crystal structure of tobacco 5-*epi*-aristolochene synthase (5-EAS), the only available structure of a plant terpene cyclase (*13*), was utilized to model a structure for AS (*14*). Although the level of homology between AS and 5-EAS is relatively low (28% identical), all plant terpene cyclases are clearly related (*15*, *16*) and are considered to assume a similar fold (*17*). Because 5-EAS does not contain an unusual ~250-residue insertional element found in AS and a few other terpenoid synthases (*15*, *16*), the modeled structure starts at His348 and depicts only the N- and C-terminal domains typical of plant terpene synthases (Figure 2). The model indicates that the $DXDD_{402-405}$ motif, required for protonation-initiated cyclization, and the highly conserved $DDXXD_{621-625}$ motif, required for diphosphate ionization-dependent reactions (*6*), are each located at the respective opening of a central cavity in the N-terminal and C-terminal helical barrel domains. These locations suggest that these cavities represent the active sites for the two sequential reactions mediated by the respective DXDD and DDXXD aspartate-rich motifs.

Mutational analysis was used to probe the putative active site for the protonation-initiated cyclization. The aspartates comprising the DXDD motif were mutated to both glutamate and asparagine, and all of the charged and aromatic residues lining the putative active site (see Figure 5) were mutated to alanine. Kinetic analysis of these mutants, with GGPP or

Table 1: Kinetic Analysis of Mutants and of the Requirement for Divalent Metal Ions[a]

	GGPP			CPP		15-aza-GGPP
	K_M (μM)	K_{si} (μM)	k_{cat} (s^{-1})	K_M (μM)	k_{cat} (s^{-1})	K_i (nM)[b]
WT with Mg^{2+}	3 ± 2	5 ± 2	2.2 ± 0.3	0.4 ± 0.2	2.2 ± 0.3	0.25 ± 0.1
WT without Mg^{2+}	20	0	2×10^{-3}	10	9×10^{-6}	ND[c]
W358A	0.4	20	2×10^{-3}	0.4	2	6
D361A	0.8	20	2×10^{-2}	0.4	2	0.4
R365A	2	6	0.2	0.7	2	0.3
D402A	1	4	3×10^{-5}	0.3	2	ND[c]
D402E	1	10	0.2	0.5	2	0.1
D402N	ND[c]	ND[c]	1×10^{-5}	0.3	2	ND[c]
D404A	7	0	2×10^{-5}	0.4	2	ND[c]
D404E	ND[c]	ND[c]	1×10^{-4}	0.3	2	ND[c]
D404N	ND[c]	ND[c]	2×10^{-5}	0.2	2	ND[c]
D405A	3	0	8×10^{-5}	0.4	2	ND[c]
D405E	1	90	4×10^{-3}	0.5	2	1
D405N	0.6	9	0.1	0.7	2	0.2
R411A	2	9	0.5	0.2	2	0.1
R454A	1	20	0.2	0.5	2	ND[c]
E499A	2	>100	2×10^{-3}	0.5	2	40
Y520A	3	20	0.1	0.5	2	0.2

[a] Kinetic constants are accurate to within ±50% of the reported value. [b] Apparent inhibition constant determined as previously described (*6*). [c] Not determined.

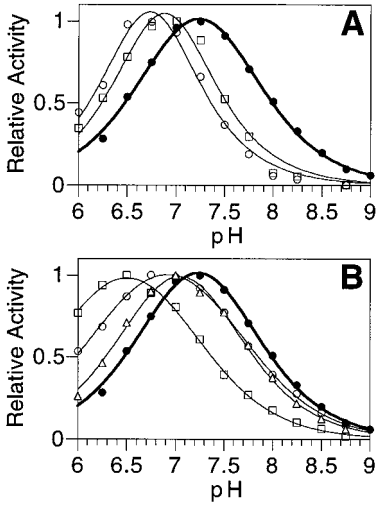

FIGURE 4: Effect of mutations on the pH dependence of AS activity. (A) Comparison of WT (●) with D402E (○) and D405E (□). (B) Comparison of WT (●) with D405N (○), E499A (□), and Y520A (△). The curves for W358A, D361A, R365A, R411A, and R454A were indistinguishable from that of WT.

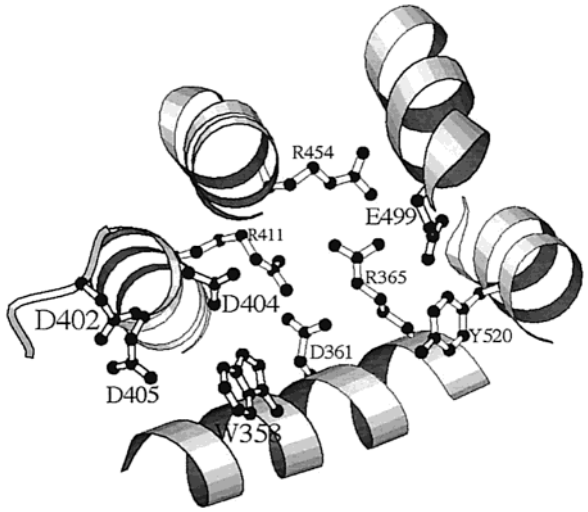

FIGURE 5: Putative active site for the protonation-initiated cyclization reaction of abietadiene synthase; the size of the label corresponds to the depth in the plane. This figure was created using Molscript (*24*).

CPP as the substrate, clearly indicated a selective effect on the protonation-initiated cyclization. The ionization-dependent reaction with CPP was essentially unaffected in every case (Table 1), and none of the mutations affected the distribution of olefinic products that arises from alternate deprotonations of the terminal abietenyl carbocation intermediate of the second reaction (from CPP) (*5*). Essentially all of the substitutions affected only the catalytic rate and not productive binding of GGPP (Table 1); changes in K_M were less than 1 order of magnitude in all cases, whereas decreases in k_{cat} ranged from 4-fold to >5 orders of magnitude (Table 1). Interestingly, many of the mutants also exhibited a reduced level of substrate inhibition with GGPP (K_{si}), with effects ranging from a slight increase in K_{si} to the complete absence of detectable inhibition (Table 1), thereby suggesting a substantial influence on the nonproductive binding mode of GGPP. None of the mutants formed abortive cyclization products or derivatives of CPP (e.g., hydroxy-CPP) from GGPP, indicating that water was effectively excluded from the active site, as with the wild-type enzyme.

All mutant enzymes that retained readily measurable levels of activity ($k_{cat} > 10^{-3}$ s^{-1}) were analyzed for changes in response to pH. For each such mutation in the DXDD motif, the activity curve was shifted downward in pH (Figure 4). For both D402E and D405E, this effect was reflected in a specific decrease in the observed right side pK_a (i.e., that approximating the pK_a of the acid), which was reduced from 7.5 to 6.5 and 6.8, respectively, without affecting the observed left side pK_a (Figure 4A). However, for D405N, this influence was reversed, and the observed shift reflected a specific decrease in the left side pK_a (i.e., that approximating the pK_a of the base), which was reduced from 7.0 to 6.2; the right side pK_a was unaffected. The only other mutants to show such effects were E499A and Y520A, in which the left side pK_a (∼base) decreased to 5.9 and 6.7, respectively, and the right side pK_a (∼acid) decreased only slightly to 7.1 and 7.4, respectively (Figure 4B). These results suggest that

these residues directly influence the groups acting as the acid and/or base.

To further examine the role of the targeted residues, the affinity of these mutants for the transition state analogue inhibitor 15-aza-GGPP was also determined. Only D405E, W358A, and E499A exhibited significant influence in exhibiting 4-, 24-, and 160-fold increases in K_i^{GGPP}, respectively, while the K_M values remained relatively constant (Table 1). These results suggest that these mutant enzymes may be impaired in their ability to stabilize the initial carbocationic intermediate arising from protonation of GGPP.

DISCUSSION

The difference between the pH−activity profile with GGPP or CPP as the substrate (Figure 3) clearly demonstrates the kinetic distinction between the diphosphate ionization-dependent cyclization from CPP and the protonation-initiated cyclization as determined by the overall rate of the reaction from GGPP. Earlier mechanistic studies demonstrated that cyclization to CPP is initiated by addition of an external proton to C14 of GGPP followed by removal of a proton from the C19 methyl group of the substrate (Scheme 1) (*10*). The rate-limiting step in this reaction was presumed to be the initial protonation catalyzed by an acidic residue of AS. However, the pH−activity profile of the overall reaction with GGPP (Figure 3) is consistent with an acid−base cyclization mechanism, indicating that a base, and an acid, are involved in the rate-limiting step(s). For a basic group to be involved in the rate-limiting step, it must either be deprotonated to relieve substrate inhibition, catalyze deprotonation of the copalyl carbocation, or stabilize the intermediate transition state. The relief of substrate inhibition with increasing pH might suggest the involvement of this nonproductive binding mode in the observed activity profile. However, there is no correlation between changes in the substrate inhibition constant and the corresponding pH−activity profiles of the mutants studied here (cf. Table 1 and Figure 4), thus leaving deprotonation or transition state stabilization as a rationale for the base-dependent slow step between which the available evidence cannot distinguish. Interestingly, the ability of various substitutions of D405 to affect either the "basic" (D405N) or "acidic" (D405E) pK_a (Figure 4) suggests cross-talk between the acid and base, implying that both are involved in a "concerted" protonation−deprotonation event or in stabilization of a single transition state.

AS requires a divalent metal ion cofactor, which was presumed to reflect a role in the diphosphate ionization-dependent reaction, because most other terpene synthases of this type exhibit a similar requirement (*9*). Therefore, it was unclear if there was any role for a divalent metal ion in the protonation-initiated cyclization step. As anticipated, the cyclization and rearrangement of CPP to abietadienes catalyzed by AS does critically depend on the presence of magnesium ion (Table 1). In addition, the protonation-initiated cyclization of GGPP to CPP also exhibited divalent metal ion dependence. There was a significant decrease in affinity for GGPP in the absence of Mg^{2+}; however, the largest effect, by far, was the 1000-fold decrease in the catalytic rate, although this effect falls short of the absolute requirement exhibited for the diphosphate ionization-dependent step of the reaction cycle (Table 1). Metal ions are not known to play a direct role in proton transfer reactions, but they are known to be involved in the binding of prenyl diphosphate substrates to terpenoid synthases (*9*) and prenyltransferases (*11*) via chelation involving aspartate (or glutamate) residues and the diphosphate moiety. Therefore, it seems likely that the substantial rate enhancement mediated by the divalent metal ion for this reaction is due to the binding and precise positioning of the GGPP substrate via the diphosphate group (which does not participate directly in catalysis in this first reaction). However, the primary structural basis for this effect is not yet known, nor was it possible, in the absence of any detailed structural information, to assign a role in catalysis of the protonation-initiated cyclization to any AS residues other than the DXDD motif.

Modeling AS against the structure of tobacco 5-*epi*-aristolochene (*13*) indicated that the $DXDD_{402-405}$ element [previously shown to be involved in protonation-initiated cyclization (*6*)] resides at the central cavity of the helical barrel N-terminal domain which forms a polar groove comprising this first active site (Figure 5). The DXDD motif is located at the top of an α-helix that is part of the barrel and is at one end of the groove. Of the three aspartates in this primary sequence element, only D404 actually protrudes into the active site; D402 and D405 are behind the helix and within hydrogen bonding distance of each other. This positioning of these aspartates is reminiscent of the active site location of a similar motif in the structure of distantly related triterpene cyclases which also catalyze a protonation-initiated cyclization, and wherein the equivalent aspartate (to D404) acts as the proton donor (*18*). W358 is located directly opposite D404 on the other side of the groove, with the D361 site further down the groove on the same side. On the floor of the groove are three arginine residues, R365, R411, and R454. E499 and Y520 are located at the other end of the groove. All of these residues were mutated to alanine to investigate their possible roles in the reaction. Additionally, the aspartates in the DXDD motif were substituted with glutamate or asparagine in an attempt to recover activity and elucidate their catalytic roles. The putative active site does not bear an obvious metal binding site (other than potential chelation by D404, D361, or E499), nor does the modeled structure offer any obvious means of excluding water from this active site to shield highly reactive carbocationic intermediates from solvent capture. However, it seems plausible that an N-terminal insertional element (Figure 2), which is present in all plant terpene synthases that catalyze similar protonation-initiated cyclizations (*15*, *16*), may serve this function. Preliminary truncation analysis of AS indicates a requirement for the insertional element in the protonation-initiated cyclization (R. J. Peters, O. A. Carter, and R. B. Croteau, unpublished results) and suggests a role for this heretofore functionally cryptic domain.

Kinetic analysis of these mutant enzymes, using either GGPP or CPP as the substrate, confirmed their specific influence on the rate of the protonation-initiated cyclization of GGPP to CPP (Table 1). None of the mutations had any significant effect on the kinetics (or product distribution) of the second, diphosphate ionization-dependent, step. Surprisingly, none of the mutations had large effects on the observed Michaelis constant for GGPP (Table 1), which may reflect limited involvement in substrate binding. However, it has previously been demonstrated that K_M is not a good ap-

proximation of the true substrate binding constant for related sequiterpene cyclases (*19*). In the case of AS, actual effects on substrate binding affinity may be similarly masked. In contrast, many of the mutants were less sensitive to substrate inhibition by GGPP, thereby demonstrating that the corresponding residues do influence the nonproductive binding mode (Table 1).

Distal ends of the putative active site can be roughly defined by the presence of both an acidic and aromatic residue, with D404 and W358 at one end and E499 and Y520 at the other (Figure 5). This placement suggests that the acidic residue may act as the acid or base, with carbocation stabilization mediated by the nearby aromatic side chain. We note that only mutations at distal ends of the putative active site significantly alter the observed pH−activity profile (Figure 4), and suggest that these changes may arise, at least in part, from effects on the actual groups which function as the acid or base. However, because interpretation of changes in the pH−activity profile of AS is complicated by the complex interaction between binding, substrate inhibition, and catalysis (all of which vary with pH), correlation of mutational change with a specific role in catalysis is not straightforward. Binding of the transition state analogue 15-aza-GGPP is also substantially altered by only mutations at the distal ends of the active site (Table 1). Interpretation is again complicated, however, because these alterations in binding could arise from interactions with any part of the analogue and so obscure precise assignment of catalytic function in the absence of detailed, experimentally determined, structural information.

All aspartates of the DXDD motif seem to be absolutely required (Table 1), as might be expected on the basis of the occurrence of this conserved element in both diterpene and triterpene cyclases which catalyze protonation-initiated cyclizations. In the present case, the middle aspartate (D404) cannot be functionally substituted, perhaps indicating that D404 acts as the acid as demonstrated for the aspartate occupying this position (and a similar active site location) in the homologous DXDD motif of a bacterial squalene-hopene cyclase (*18*). Interestingly, the results of glutamate and asparagine substitution of these aspartates in AS contrast with those obtained for similar mutations in squalene-hopene cyclases. In these latter cases, only the middle, but not the first or last, aspartate could be functionally substituted (*20*, *21*), whereas for AS the opposite is true (i.e., the middle aspartate cannot be functionally substituted, but the others can be). These contrasting results imply a precise requirement for the position of the D404 carboxyl side chain, and may indicate a different role for the DXDD motif in AS compared to the triterpene cyclases (i.e., as the base rather than the acid). Because all mutants of the DXDD aspartates do not significantly affect K_M, while profoundly affecting k_{cat}, this sequence element does not seem to be involved in substrate binding via metal ion chelation (a role ascribed to the superficially related DDXXD motif associated with ionization-dependent cyclizations).

Alanine substitution for arginines in the putative active site had a relatively small effect (Table 1). However, these mutant enzymes may be structurally compromised, because the level of soluble protein expression was decreased by at least one order of magnitude relative to that of either wild-type rAS or other mutants. Finally, while D361 seemingly plays an important role in catalysis (Table 1), the role of this residue is unclear. D361 could serve to stabilize an intermediate carbocation; however, D361A did not yield abortive cyclization products as might be anticipated for modification of a residue involved in such stabilization.

In addition to (−)-copalyl diphosphate synthases of the gibberellin biosynthetic pathway (*22*), levopimaradiene synthase from *Ginko biloba* has recently been cloned and functionally expressed (*23*). Each of these diterpene synthases catalyzes a protonation-initiated cyclization very similar to that of AS. Alignment of these sequences with that of AS demonstrated the highly conserved nature of the putative active site residues described here, as well as the presence and similar placement of the insertional element; these features are not conserved in diterpene synthases which do not catalyze protonation-initiated cyclizations (*15*, *16*). Of the residues examined in this study, only R411 and Y520, which do not seem to play critical roles in catalysis, are not completely conserved but do exhibit conservative substitutions (Lys and Phe, respectively). This degree of conservation at the presumptive active site suggests that these residues may serve similar functions in a common mechanism for diterpene protonation-initiated cyclization.

In summary, we have presented a detailed assessment of the protonation-initiated cyclization reaction catalyzed by AS. Analysis of the pH dependence of the overall reaction demonstrates an acid−base catalytic mechanism and, unexpectedly, indicates that a basic residue participates in a rate-limiting step involving deprotonation or transition state stabilization. Analysis of the dependence of this reaction on divalent metal ions demonstrates a dramatic influence on catalytic efficiency, although the mechanistic and structural bases of this effect are not clear. Mutational analysis of the putative active site for this first step in the reaction cycle strongly supports catalytic roles for many of the charged and aromatic residues targeted in the modeled structure. The ability of the modeled structure to accurately predict this nonconserved active site, despite the relatively low level of homology between AS and 5-EAS, further validates previous suggestions that all terpene cyclases assume similar structural folds (*13*, *17*). Further consideration of the model also suggests a role in solvent shielding for the functionally cryptic insertional element of this enzyme. The highly conserved nature of residues in the putative active site (and the presence of the insertional element) in all similar diterpene synthases suggests a common reaction mechanism for the protonation-initiated cyclization step; however, a crystal structure will be required to permit more precise definition of catalytic function.

ACKNOWLEDGMENT

We thank Dr. E. Davis for assistance with the modeling and for productive discussions and G. Selhorn, III, for technical assistance with mutant construction.

REFERENCES

1. Phillips, M. A., and Croteau, R. B. (1999) *Trends Plant Sci. 4*, 184−190.
2. Johnson, M., and Croteau, R. (1987) *Am. Chem. Soc. Symp. Ser. 209*, 76−92.
3. Funk, C., and Croteau, R. (1994) *Arch. Biochem. Biophys. 308*, 258−266.

4. LaFever, R. E., Stofer Vogel, B., and Croteau, R. (1994) *Arch. Biochem. Biophys. 131*, 139−149.
5. Peters, R. J., Flory, J. E., Jetter, R., Ravn, M. M., Lee, H.-J., Coates, R. M., and Croteau, R. B. (2000) *Biochemistry 39*, 15592−15602.
6. Peters, R. J., Ravn, M. M., Coates, R. M., and Croteau, R. B. (2001) *J. Am. Chem. Soc. 123*, 8974−8978.
7. Duncan, J. D., and West, C. A. (1981) *Plant Physiol. 68*, 1128−1134.
8. Saito, T., Abe, H., Yamane, H., Sakurai, A., Murofushi, N., Takio, K., Takahashi, N., and Kamiya, Y. (1995) *Plant Physiol. 109*, 1239−1245.
9. Davis, E. M., and Croteau, R. (2000) *Top. Curr. Chem. 209*, 53−95.
10. Ravn, M. M., Coates, R. M., Jetter, R., and Croteau, R. (1998) *J. Chem. Soc., Chem. Commun.*, 21−22.
11. Koyama, T., and Ogura, K. (1999) in *Isoprenoids Including Carotenoids and Steroids* (Cane, D. E., Ed.) pp 69−96, Elsevier Science, Oxford, U.K.
12. Stofer Vogel, B., Wildung, M. R., Vogel, G., and Croteau, R. (1996) *J. Biol. Chem. 271*, 23262−23268.
13. Starks, C. M., Back, K., Chappell, J., and Noel, J. P. (1997) *Science 277*, 1815−1820.
14. Peitsch, M. C., and Guex, N. (1996) *Biochem. Soc. Trans. 24*, 274−279.
15. Bohlmann, J., Meyer-Gauen, G., and Croteau, R. (1998) *Proc. Natl. Acad. Sci. U.S.A. 95*, 4126−4133.
16. Trapp, S. C., and Croteau, R. B. (2001) *Genetics 158*, 811−832.
17. Lesburg, C. A., Zhai, G., Cane, D. E., and Christianson, D. W. (1997) *Science 277*, 1820−1824.
18. Wendt, K. U., Poralla, K., and Schulz, G. E. (1997) *Science 277*, 1811−1815.
19. Mathis, J. R., Back, K., Starks, C. M., Noel, J., Poulter, C. D., and Chappell, J. (1997) *Biochemistry 36*, 8340−8348.
20. Feil, C., Sussmuth, R., Jung, G., and Poralla, K. (1996) *Eur. J. Biochem. 242*, 51−55.
21. Sato, T., and Hoshino, T. (1999) *Biosci., Biotechnol., Biochem. 63*, 2189−2198.
22. Sun, T.-P., and Kamiya, Y. (1994) *Plant Cell 6*, 1509−1518.
23. Schepmann, H. G., Pang, J., and Matsuda, S. P. (2001) *Arch. Biochem. Biophys. 392*, 263−269.
24. Kraulis, P. J. (1991) *J. Appl. Crystallogr. 24*, 946−950.

BI011879D